Gravity changes and passive SO2 degassing at the Masaya caldera complex, Nicaragua

Gravity changes and passive SO_2 degassing at the Masaya caldera complex, Nicaragua

Glyn Williams-Jones♂, Hazel Rymer and David A. Rothery

Volcano Dynamics Group, Department of Earth Sciences, The Open University, Walton Hall, Milton Keynes, MK7 6AA, UK

♂Corresponding author: Glynwj@higp.hawaii.edu
Present address: Hawaii Institute of Geophysics & Planetology, SOEST, University of Hawaii, Honolulu, Hawaii 96822, USA

Abstract

An understanding of the mechanisms responsible for persistent volcanism can be acquired through the integration of geophysical and geochemical data sets. By interpreting data on micro-gravity, ground deformation and SO_2 flux collected at Masaya volcano since 1993, it is now clear that the characteristic cyclical nature of activity is not driven by intrusion of additional magma into the system. Rather, it may be due in large part to the blocking and accumulation of gas by restrictions in the volcano substructure. The history of crater collapse and formation of caverns beneath the crater floor would greatly facilitate the trapping and storage of gas in a zone immediately beneath San Pedro and the other craters. Another mechanism that may explain the observed gravity and gas flux variations is the convective overturn of shallow, pre-existing, degassed, cooled, dense magma that is replaced periodically by lower density, hot, gas-rich magma from depth. Buoyant gas-rich magma rises from depth and is emplaced near the surface, resulting in the formation and fluctuation of a low-density gas-rich layer centred beneath Nindirí and Santiago craters. As this magma vigorously degasses, it must cool, increase in density and eventually sink. Five stages of activity have been identified at Masaya since 1853 and the most recent data suggest that the system may have been entering another period of reduced degassing in 2000. This type of analysis has important implications for hazard mitigation because periods of intense degassing are associated with poor agricultural yields and reduced quality of life. A better understanding of persistently, cyclically active volcanoes will allow for more effective planning of urban development and agricultural land use.

Keywords: Masaya; micro-gravity; passive degassing; persistent activity; convection

Introduction

Located in western Nicaragua, Masaya (635 m a.s.l.) is a persistently active basaltic shield volcano and caldera complex (Fig. 1). Thought to have formed between ~6500 and 2250 BP by a series of large basaltic ignimbrite eruptions (8-12 km^3), Masaya caldera is believed to be underlain by a 10 km^3 open-system magma reservoir at shallow upper-crustal depths (Williams, 1983a, b; van Wyk de Vries, 1993; Walker et al., 1993). A basaltic edifice has developed within the caldera from eruptions along an arcuate series of vents. The main edifice-building activity resulted in the formation of the Masaya and Nindirí cones, and several episodes of pit crater collapse have led to the development of the Masaya, Santiago, Nindirí and San Pedro pit craters (Fig. 1b). The currently active Santiago crater is believed to have formed in 1859 (McBirney, 1956; Rymer et al., 1998). A static Bouguer gravity survey carried out between 1991 and 1992 across the caldera revealed a large positive anomaly off centre with respect to the main axis of the caldera and thought to indicate a dense relatively shallow body (2-3 km b.s.l.) emplaced prior to caldera formation (Métaxian, 1994). There is no significant Bouguer gravity anomaly associated with the present magma system and current activity at Santiago crater. However, seismic and magnetotelluric studies do indicate the presence of a very shallow magma body resident immediately beneath the floor of Santiago crater, while volcano-tectonic earthquake hypocentres are generally at depths of ~1 km b.s.l. (Métaxian, 1994; Métaxian et al., 1997).

Prolonged episodes of passive degassing and oscillations in the level of the magma column are characteristic of activity at Santiago crater during which the top of the magma column is occasionally visible within the vent or rises to form a lava lake. There may have been at least five cycles of degassing and frequent changes in the magma column height since the formation of Santiago crater in 1859 (Stoiber et al., 1986; Rymer et al., 1998). The most recent cycle of activity began in May 1993 and continues to the present (BGVN, 1970-2001;

Rymer et al., 1998). An excellent means of studying this activity is through the integration of SO_2 flux measurements by ultraviolet correlation spectrometry (COSPEC) and dynamic micro-gravity surveys.

Methodology

Dynamic micro-gravity and deformation

Subsurface mass and density changes within a volcano can be quantified and located using a combination of high-resolution ground deformation and micro-gravity monitoring techniques. Dynamic or "relative" micro-gravity monitoring involves the measurement of small gravity changes with time and space across a network of stations. The theory and field practice for volcano micro-gravity monitoring has been discussed fully in the literature (cf. Rymer and Brown, 1989; Rymer, 1996) and therefore will only be summarised briefly. We have increased the monitoring network, initially installed at Masaya by S. Bonvalot (Institut pour la Recherche et le Dévevoplement), Métaxian (1994) and Rymer et al. (1998), to 38 stations across the caldera (Fig. 1a, 2). For this study, micro-gravity measurements were made during six field campaigns (Jan. 1998, Sept. 1998, Feb. 1999, June 1999, Mar. 2000 and Feb. 2001) using the LaCoste and Romberg gravity meter G513. Importantly, this is the same instrument as used by Rymer et al. (1998) for measurements between 1993 and 1997. Aside from one discrete change in 1994/95, the instrument calibration factor for G-513 has remained stable for the period of this study (Carbone and Rymer, 1999). Gravity values are quoted relative to the reference or field base station, A1, which has previously been assumed to be outside the area of gravity variation (Fig. 1a, 2; Rymer et al., 1998). In order to confirm that gravity at this base station remains stable, a series of four secondary reference stations was installed outside the caldera in 1998 (Regis) and 1999 (LaClinica, ParqueSM, EstacionT), at distances of up to 15 km from the active craters (Fig. 1a). All raw gravity

measurements have been corrected for the effects of solid Earth tides using software developed by Broucke et al. (1972).

It is frequently possible to achieve micro-gravity measurements at high precision (±10 μGal) at volcanoes when following strict survey procedures (Rymer and Brown, 1989). However, in the case of Masaya, the continuous degassing-induced volcanic tremor (Métaxian et al., 1997) and potential for temporary "tares" from this seismic noise (Davies et al., 2000) make precise measurements difficult. Therefore, the uncertainty in a single

$$\sqrt{20^2 + 10^2} \approx 22 \qquad (1)$$

measurement is generally estimated at ±20 μGal. In fact each measurement is "normalised" to a very stable, [illegible] μGal, Fig. 1). Thus, the uncertainty for a given gravity measurement (e.g., A7 – A1) would be:

$$\sqrt{\left(20^2 + 10^2\right)} \approx 22\mu Gal \qquad (1)$$

Furthermore, each gravity difference has actually been measured up to 5 times during each survey.

Seasonal effects can produce significant apparent gravity change principally because of ground water depth variations. Indeed, this effect has been noted at a number of other volcanoes (e.g., ±4 μGal at Long Valley, Jachens and Roberts, 1985; 40-60 μGal at Mt. Etna, Rymer et al., 1995). However, at Masaya the effects are almost negligible because the water table is at a depth of at least 300 m (Krásný and Hecht, 1998). Furthermore, for consistency and ease of measurement, field campaigns were generally carried out during the dry season (January to April). Of the two field campaigns carried out during the wet season (October 1994 and June 1999), neither showed any detectable seasonal effect (gravity continued to decrease at a similar rate to that of the previous and subsequent field campaigns; see below). Since then, all measurements have been made at approximately the same time every year

(February to March) to reduce any effect there may be. A seasonal effect is therefore not thought to be a significant factor in the following discussion.

Free Air Gradient measurements

Gravity varies with elevation along the Free Air Gradient (FAG) which has a theoretical value of –308.6 μGal m^{-1} at sea level. However, terrain effects and Bouguer anomalies can cause this value to differ by up to 40% from the theoretical value (Rymer, 1994 and references therein). Therefore, when possible, the actual FAG should always be measured at each station during a micro-gravity/deformation survey (Berrino et al., 1984; Yokoyama, 1989; Rymer, 1994; Jousset et al., 2000). The difference in gravity (Δg) is then divided by the difference in elevation (Δh) to obtain the FAG. In June 1999, Free Air Gradient measurements were made at 19 of the 38 network stations across the caldera (Fig. 1). As would be expected, the observed FAG at Masaya is essentially controlled by topography, ranging from –250 μGal m^{-1} at distal stations (>2 km from Santiago) up to –390 μGal m^{-1} at summit stations; the average FAG for summit stations is -340 μGal m^{-1}.

Ground deformation measurements

Ground deformation over the entire network was measured at least once every field campaign using a Leica GPS 200 dual-frequency differential receiver, following strict survey procedures (Table 1; Murray et al., 1995; Rymer, 1996). Due to technical problems, height measurements are unavailable for the June 1999, September 1999 and April 2000 campaigns. Nevertheless, measurements made since the start of measurements in 1993, suggest that elevation changes have been below the level of significance for affecting gravity measurements (<2-4 cm per annum, Table 1; Rymer et al., 1998). The typical effect of such a height change on gravity measurements is discussed below. While it is possible that there

may have been inflation and deflation of the volcano between surveys, the lack of any coherent variations in the observed elevation changes suggest that this is unlikely. Nevertheless, installation of a continuously recording GPS is the only way to determine this for sure.

For an elevation change of 2 cm yr^{-1}, the effect on gravity would range from –5 to –8 μGal yr^{-1} which is not detectable. The maximum size of any height correction would be ~16 μGal (for a 4 cm elevation change at a maximum measured FAG of -390 μGal m^{-1}), while a calculated Bouguer-corrected free air gradient of -317 μGal m^{-1} would result in a maximum correction of ~12 μGal. Given the lack of any recent significant extrusive events or elevation changes and the periods of large gravity variation (~70 μGal yr^{-1}), there has been no reason to height-correct our micro-gravity data. Gravity changes are therefore interpreted here in terms of subsurface mass or density variations.

SO_2 gas flux

A valuable means of studying the current degassing episode at Masaya is through the use of a COSPEC that allows for the measurement of SO_2 flux, expressed as metric tonnes per day (t d^{-1}). For this study, the COSPEC was mounted in a vehicle and repeatedly driven along routes crossed by the volcanic plume, allowing for vertical scans of the plume. Detailed descriptions of the technique can be found in the literature (e.g., Millán, 1980; Stoiber et al., 1983; Casadevall et al., 1987; Williams-Jones, 2001; Williams-Jones et al., In Press). The largest source of uncertainty in COSPEC measurements is caused by the difficulties in accurately measuring the windspeed, which is used as a proxy for the speed of the gas column. However, at Masaya this uncertainty is greatly reduced as windspeed measurements are made virtually at the column height with a continuous-recording anemometer, located at an Instituto Nicaragüense de Estudio Territoriales (INETER) seismic station, 930 m a.s.l.

Generally, 10 traverses were made per day, with individual traverses lasting approximately 20-40 minutes. During the dry season (December to April), there is a relatively steady easterly trade wind, and thus COSPEC measurements typically were made to the west of the volcano, at a distance of between 4 and 15 km from the crater.

Results

Dynamic micro-gravity and deformation

As mentioned above, dynamic or "relative" micro-gravity entails relating measurements at a given station to a base station (A1 for Masaya). However, this assumes that gravity at this base station is invariant. In order to confirm this supposition, four reference stations were installed outside the caldera in 1998 and 1999, with measurements made at least once (for the more distal stations of Regis, LaClinica, ParqueSM and EstacionT) during a given field campaign (Fig. 1, 3). The first reference station, Regis, proved to be unstable with respect to A1 due probably to its location in the Hotel Regis with vibrations from the movement of the many hotel guests. However, the more distal stations generally show variations of less than 20 μGal at the 95% confidence level relative to station A1, confirming that A1 is stable with respect to the outer caldera region. This is further supported by data from the those stations located within the caldera and at least 2 km from Santiago crater, the majority of which also fall within 20 μGal of zero at a 95% confidence level. Furthermore, the lack of any consistent trends in gravity at distal stations (in contrast to those of the summit stations) suggests that the variations are not related to volcanic activity (Fig. 4). These stations are therefore not considered further.

Between February 1993 and April 1994, summit stations underwent an average gravity decrease of 95 ± 48 μGal, followed by an average gradual increase of 24 ± 24 μGal between April 1994 and March 1997 relative to station A1 (Fig. 5, Rymer et al., 1998). This

was followed by a second relatively consistent gravity decrease of 46 ± 14 μGal yr^{-1} between March 1997 and June 1999; slower but of the same order as that observed between 1993 and 1994 (Fig. 5). This is followed by an apparent "levelling off" of the gravity variations between June 1999 and February 2001.

The spatial extent of gravity change between 1993 and 1994 indicates a crater-centred negative anomaly of at least -90 μGal (Fig. 6b; Rymer et al., 1998). However, the paucity of summit stations during this period makes it difficult to fully constrain the gravity anomaly. The excellent correlation of gravity change between the summit stations (Fig. 5), irrespective of absolute amounts, can be used to better constrain the gravity anomalies. By taking a linear regression of the average monthly gravity changes of selected summit stations (1998-2001) with respect to station A7, new data can be extrapolated back in time to provide semi-quantitative insights into gravity variations around the crater (Fig. 6). Thus, between 1993 and 1994, a larger crater-centred anomaly of at least -120 μGal is suggested. As noted above, gravity increased slightly between 1994 and 1997, although the lateral extent of the anomaly is poorly constrained (Fig. 6c). Gravity decreases between 1997 and June 1999 show a very similar anomaly to that of 1993-1994, in both spatial extent and magnitude, and suggest that gravity changes remained essentially crater-centred during this period (Fig. 6d). There was no significant gravity change between June 1999 and 2001, and as with the 1994-1997 period, the anomaly is only poorly constrained (Fig. 6f). Interestingly, during periods of gravity decrease (1993-1994 and 1997-1999), the anomaly seems to be centred over Nindirí crater rather than the active Santiago crater (Fig. 6).

SO_2 Flux

The most recent degassing episode at Masaya was preceded by weak fumarolic activity (throughout the early 1990s) leading to increased degassing in May 1993 with a

"diffuse white sulphur-rich plume" observed several kilometres from Santiago crater (BGVN, 1970-2001; Rymer et al., 1998). In contrast to an April 1992 COSPEC measurement of <10 t d^{-1} (BGVN, 2000), comprehensive COSPEC monitoring started in 1996 showed moderately elevated emissions of 600 ± 290 t d^{-1} in March 1996 and 390 ± 200 t d^{-1} in February-March 1997 (Fig. 7; Rymer et al., 1998; Delmelle et al., 1999). These rates increased significantly to 1850 ± 960 t d^{-1} in 1998 and 1650 ± 560 t d^{-1} in 1999. The most recent measurements (February-March 2001) show a decrease in the average SO_2 flux to 580 ± 250 t d^{-1}. All these values are minimum for SO_2, because the measurements are affected by the presence of other sulphur species. However, work by Stoiber et al. (1986) suggests that H_2S and SO_4^{2-} (aerosol) will have only a limited effect of SO_2 flux estimates (H_2S/SO_2: 0.0006; SO_4^{2-}/SO_2: 0.093).

The rate at which magma degassed during these same periods can be estimated from the measured gas flux. Using the degassing data presented in Williams-Jones (2001), it is estimated that between 2.0 x 10^8 and 6.5 x 10^8 kg yr^{-1} of SO_2 was emitted between 1993 and 2001 (Table 2). Based on Fourier Transform Infrared (FTIR) spectroscopic measurements of the major gas species in the plume (H_2O, CO_2, SO_2, HCl and HF), the emission rate of total gas during these periods ranges from 4.3 x 10^9 to 1.4 x 10^{10} kg yr^{-1} (Williams-Jones, 2001, Table 2). Assuming reasonable initial sulphur contents (in the melt) of between 270 and 1500 ppm (Stoiber et al., 1986; Roggensack et al., 1997; Métrich et al., 1999), the minimum rate of magma degassing for these intervals varied between 6.7 x 10^{10} and 1.2 x 10^{12} kg yr^{-1} (Table 2).

Micro-gravity analysis

Subsurface mass or density changes at Masaya may be caused by (a) water-table fluctuations, (b) magma drainage or intrusion and (c) magma vesiculation or devesiculation. The first case is unlikely here because, as mentioned above, the water table is quite deep in

this area (>300 m; Krásný and Hecht, 1998) and as can be seen from Fig. 6, gravity changes are concentrated around the active crater area. Magma drainage is also unlikely since this period has been characterised by significant degassing, minor strombolian events and persistent incandescence of the active vent.

A minimum estimate of the mass change (Δm) responsible for the observed gravity changes (Δg) can be made by integrating the residual gravity change over the area (ΔS) in which it occurs. Using Gauss' theorem (Telford et al., 1990, p. 43):

$$\Delta m = \frac{1}{2\pi G} \Delta S \Delta g \qquad (2)$$

where G is the Universal Gravitational constant (6.67×10^{-11} N m^2 kg^{-2}). Note that, for the gravity change between 1998 and 1999, the actual area affected by the –60 μGal anomaly (~6.3×10^6 m^2) is equal to the total area within the –60 μGal anomaly (~8.6×10^6 m^2) minus the area affected by the –90 μGal anomaly (~2.3×10^6 m^2; Fig. 6e). Thus, the total mass change (Δm_{tot}) is equal to the sum of mass changes calculated for the –90 μGal (Δm_{90}) and –60 μGal (Δm_{60}) anomalies, where:

$$\Delta m_{90} = \frac{1}{2\pi G} 2.3 \times 10^6 \text{ m}^2 - 90 \times 10^{-8} \text{ m s}^{-2} = -5.0 \times 10^8 \text{ kg} \qquad (3)$$

$$\Delta m_{60} = \frac{1}{2\pi G} 6.3 \times 10^6 \text{ m}^2 - 60 \times 10^{-8} \text{ m s}^{-2} = -9.1 \times 10^8 \text{ kg} \qquad (4)$$

$$\Delta m_{tot} = \Delta m_{90} + \Delta m_{60} = -1.4 \times 10^9 \text{ kg} \qquad (5)$$

Ideally, one would attempt to "close" the zero μGal anomaly contour, but as this is not feasible because of the low station density of the network, only a minimum estimate of mass change is possible. In the case of gravity changes between 1997 and 1999 (Fig. 6d), the

-120 and -90 μGal contours are used giving a total mass change (Δm_{tot}) of at least -2.1 x 10^9 kg. Similarly, the 1993-1994 gravity changes (using -60, -90 and -120 μGal contours; Fig. 6b) are likely to be the result of a total mass change of at least -2.2 x 10^9 kg (Table 2).

As mentioned above, we are unable to "close" the zero of the gravity contour and thus can not compute the "real" depth and size of the magma reservoir. It is therefore sensible to use the structural evidence, such as the diameter of Santiago and Nindirí craters and their inferred boundary faults (Rymer et al., 1998), to constrain the lateral extent of the body responsible for the anomaly. However, the craters grow through erosion and collapse of the walls and so provide an overestimate of lateral extent of any single magma body. Further information regarding the subsurface geometry of the magmatic system can be obtained from the limited seismic studies of Métaxian et al. (1997) which suggest the presence of a small shallow reservoir at ~1 km b.s.l.

In this study, the implications of the observed gravity decrease anomalies (1993-1994 and 1997-1999) have been investigated using the interactive 2.5-dimension forward modelling programme GRAVMAG (Pedley, 1991). The gravitational effect of subsurface geology measurable at the topographic surface (taken from a Digital Elevation Model supplied by INETER) is calculated along a given profile. Geology is represented by a series of user-defined polygons, each assigned a density and half strike. The models are 2.5D rather than 3D, as each polygon must be symmetrical across (but not along) the profile. By modifying the physical parameters of each polygon (e.g., size, density, half strike), the calculated gravity profile can be "fitted" to the observed gravity profile.

Density changes within a feeder pipe of reasonable dimensions (e.g., tens of metres or less in diameter) would result in a Bouguer gravity anomaly of shorter wavelength than observed. On the other hand, changes within a deep magma (e.g., > 1 km b.s.l.) reservoir would produce an anomaly with a wavelength larger than the ~2 km signature observed at

Masaya (Rymer et al., 1998). In an attempt to constrain the bodies responsible for the observed gravity anomalies, north-south and west-east model profiles were initially made across the active crater, Santiago (Fig. 6a). A north-south profile of the 1993-1994 gravity decrease can be modelled in terms of changes in a stratified body approximately 490 m wide, with a 200 m half strike and 180 m stratified thickness; a 30 m upper layer of high density change (-600 kg m^{-3}) above a body of lower relative density change (-100 kg m^{-3}; Fig. 8a); this is virtually identical to that modelled by Rymer et al. (1998). A west-east profile for the same period suggests changes in a body of similar dimensions, as it should (450 m wide, 30 m thick at -600 kg m^{-3} and 150 m thick at -100 kg m^{-3}; Fig. 8b). The 1997-1999 gravity anomaly can also be modelled in terms of a stratified body, though with different density changes. The north-south and west-east profiles indicate a body between 465 and 560 m wide with three layers (20 to 90 m thick) with densities changes ranging from -300 to –100 kg m^{-3} (Fig. 8c,d). Modelling of the 1998-1999 gravity anomaly, which is based on a larger number of measurements, supports the 1997-1999 model (Fig. 8e, f).

The west-east profiles for 1993-1994 and 1997-1999 may alternatively be modelled in terms of two causative bodies (though with different density changes) and suggest that some of observed density changes within the system are centred beneath Nindirí crater (Fig. 8g, h). In order to investigate this further, an oblique profile running NW-SE across the craters was made for the 1998-1999 period (Fig. 6a, 9). Modelling of these data, although limited by the lack of data for the floors of San Pedro and Santiago pit craters, suggests that there may be areas of density change (-100 kg m^{-3} for 1998-1999) beneath the entire pit crater complex. It is unlikely that the actual shape of the causative bodies has changed significantly between 1993 and the present. Rather, the small differences in modelled sizes are likely to be the result of uncertainties in gravity measurements. However, the variations in density change over the measurement period are clearly significant.

As suggested by Rymer et al. (1998), these modelled density changes can be best explained by changes in the degree of vesiculation. The 1993-1994 model suggests that there was an ~20% increase in vesiculation in an upper layer and ~5% vesiculation change in a lower layer. Similarly, the 1997-1999 model may be the result of an ~12% change in the degree of vesiculation in an upper layer, grading through a 10% change in the middle layer to a ~5% change in vesiculation in a lower layer.

It is important to note that the lack of measurements on the crater floors (i.e., the areas with the greatest likely gravity anomalies) reduces the level to which the modelled gravity profile can be "fitted" to the observed data (Fig. 8). This greatly limits the extent to which these causative bodies can be confidently modelled.

Interpretation

Modelling of the gravity anomalies is limited by the rather poor spatial resolution and geographic coverage of the data. However, the most likely cause of the observed gravity variations is a change in density of a region of stratified vesiculated bodies located immediately beneath Santiago, Nindirí and San Pedro craters (Fig. 8, 9, and 10). A four-stage model can be used to explain the observed fluctuations in micro-gravity and gas flux, with Stage 1 being arbitrarily set at the beginning of significant degassing in May 1993 (Fig. 11). The initial state of the vesiculated region, during Stage 0, is unknown. However, the low SO_2 flux in April 1992 from COSPEC measurements (<10 t d^{-1}; BGVN, 1970-2001) suggests that it was probably relatively thin. We interpret the significant gravity decrease during Stage 1 (May 1993-1994) as having been caused by the thickening of a low-density vesiculated layer (above higher-density magma) in response to elevated gas flux (Fig. 11; (Rymer et al., 1998). This body may have effectively thickened the existing vesiculated region by ~200 m. With a reduction in gas flux, this vesiculated layer stabilised or may have thinned somewhat during

Stage 2 (1994-1997). Subsequently, a significant increase in gas flux between 1997 and 1998 may have coincided with a thickening of this low-density zone (again to ~200 m thicker than before), causing the gravity decrease observed during Stage 3 (1997-June 1999). Finally, levelling off of the gravity change during Stage 4 (June 1999 to present) may be related to a decrease in gas flux and therefore stabilisation of the low-density layer once again (Fig. 11). However, this can only be clarified by ongoing gravity and gas flux measurements.

The estimated total gas flux in Stage 1 (4.7×10^9 kg yr^{-1}) is coincidentally of the same order of magnitude as the estimated mass decrease (2.2×10^9 kg) responsible for observed gravity changes (Table 2). However, the estimated total gas flux in Stage 3 is significantly greater than that estimated from gravity measurements (1.0×10^{10} kg yr^{-1} vs. 2.1×10^9 kg), while 1998-1999 gas flux is an order of magnitude greater (1.4×10^{10} kg yr^{-1} vs. 1.4×10^9 kg). This suggests that the mass change estimated by micro-gravity is not directly related to the amount of gas released or amounts of magma degassed but instead must be largely attributable to changes in vesicularity within an open system.

The similarity of model suggested above to the model of bubble accumulation proposed by Jaupart and Vergniolle (1989) raises the possibility that bubble accumulation and formation of a foam layer may also be occurring deeper, at the roof of the shallow reservoir. The generally consistent SO_2 flux rates at Masaya may in fact be indicative of a steady foam flow regime (Jaupart and Vergniolle, 1989) in which persistent degassing causes bubbles to accumulate as a “permanent” foam layer that flows along the roof of the reservoir and escapes into the conduit. While development of a foam at shallow or deep levels may influencing persistent activity at Masaya, the mechanism responsible for changes in the degassing rate must be explained.

Convection in the crater feeder conduit has been proposed as a mechanism for removing the degassed magma (Kazahaya et al., 1994; Rymer et al., 1998; Stevenson and

Blake, 1998). The fate of this degassed magma remains uncertain. Two end-member models have been suggested: 1) intrusion into the edifice or cryptically beneath the volcano and 2) recycling back into the underlying magma reservoir (Harris et al., 1999 and references therein). In the case of Masaya, edifice and/or cryptic intrusion of the degassed magma are unlikely as this would result in inflation and gravity increase, neither of which has been observed.

Initially at Masaya, gas-rich magma would rise buoyantly towards the surface where it would degas, cool, crystallise and become denser, before descending the conduit. Gas flux data suggest that during Stage 1, magma degassed at a minimum rate of between 7.3×10^{10} and 4.1×10^{11} kg yr^{-1} and increased to 1.2×10^{12} kg yr^{-1} in Stage 3 (Table 2). Assuming a magma density of 2600 kg m^{-3}, these are equivalent to degassed magma volumes of between 0.03 and 0.5 km^3 yr^{-1}. The degassed magma must therefore be recycled back into the underlying magma reservoir.

The rate at which this magma is recycled may be inferred to some degree from the micro-gravity and gas flux data. After the initial rise of gas-rich magma and formation of the vesiculated layer beneath Santiago and Nindirí in Stage 1 (~1.5 years), the rate of degassing decreased progressively over a period of approximately 2.5 years (Stage 2) resulting in a stabilisation or slight increase in gravity. The slight increase in gravity may be a response to a number of factors, including: 1) density increase of the degassed magma; 2) the replacement of vesiculated magma by less vesicle-rich magma; 3) a slight thinning of the low-density layer or reduction in its vesicularity, or 4) escape of gas through the vent at a rate faster than it can be replenished from below. This period was followed by the renewal of elevated degassing and progressive gravity decrease over a period of ~2.5 years (Stage 3). Data from June 1999 onwards suggest that the system may have entered another period of decreased

degassing and stabilisation of gravity (Stage 4). It is clearly presumptuous to predict the duration of Stage 4, but it may be of the same order as Stage 2.

Thus, in summary, gas-rich magma may have risen to the surface in early 1993 and degassed over a period of ~1.5 years, releasing sufficient gas to thicken any pre-existing low-density vesicular area. The apparent stabilisation of the low-density area and decreasing gas flux in Stage 2 suggest that the degassed, dense magma may have sunk downwards. This would have been followed by convective overturn at depth of new or recharged gas-rich magma that then rose buoyantly to the surface during Stage 3, releasing gas and thickening the shallow low-density area. The decreasing gas flux and negligible gravity change from July 1999 onwards (Stage 4) suggest that this magma may have degassed, increased in density and begun to descend. This convective overturn should not be thought of as a series of individual events but rather as a continuous process with the rise, degassing and sinking of magma, at least during a given degassing episode (e.g., since 1993). Similar activity may also have been responsible for the variations in SO_2 flux observed during the 1979-1989 degassing episode at Masaya (Stoiber et al., 1986).

This raises the important question of whether the periods between degassing episodes are indicative of the rates of convection within the deeper source region. In many cases the magma eruption rate at a volcano is used as a proxy for the magma supply rate (cf. (Denlinger, 1997). However, as only negligible amounts of magma have been erupted at Masaya, the magma-degassing rate may also be used as a proxy (Francis et al., 1993). With a time-averaged SO_2 flux (1972-2001) of $4.3 \pm 2.7 \times 10^8$ kg yr^{-1} (Williams-Jones, 2001), magma could be supplied from depth, to the shallow (~1 km b.s.l.) magma reservoir at a rate on the order of $2 - 7 \times 10^{11}$ kg yr^{-1}. Unfortunately, the near-complete lack of erupted material makes it difficult to determine (through decay-series disequilibria methods; cf. Pyle, 1992) the residence time of magma in the shallow reservoir and deeper source. However, recent

work at Stromboli using short-lived disequilibria of ^{210}Pb-^{210}Bi-^{210}Po in volcanic gases has enabled an estimate of magma residence time in the upper reservoir (Gauthier et al., 2000). This, in conjunction with continued long-term geophysical monitoring, has the potential to better constrain the rate of convection at the different levels of the magmatic system beneath Masaya.

The magmatic system of Masaya

While the shape of both the shallow and deep magmatic systems of Masaya is unknown, several suppositions can be made. Pit craters such as Santiago and San Pedro vary in size due the wall collapse and floor subsidence (Rymer et al., 1998), suggesting that the immediate area beneath the crater floor is likely a chaotic region of gas/magma-filled voids interspersed with sunken crater wall/floor material (Fig. 10). This is supported by the visual observations of unroofing of small "caverns" (5-30 m diameter) located beneath the crater floor of Santiago (Rymer et al., 1998). Blockage of these small caverns likely results in the infrequent vent-clearing explosions. Such an event occurred recently on April 23, 2001 with the old vent ceasing to be active and a new one opening only a few meters away (BGVN, 2001). These voids may also allow for the accumulation of gas and result in the "puffing" (on the order of tens of seconds), characteristic of degassing at Santiago. Furthermore, the spatially restricted (i.e., small wavelength) micro-gravity anomalies of 1993-1994 and 1997-1999 (Fig. 6), suggest that significant density changes are occurring at shallow levels (<200 m below the crater floor), centred on and in the immediate vicinity of Nindirí crater. Below this, earthquake hypocentre data suggest the presence of a small shallow reservoir at ~1 km b.s.l. (Fig. 2; Métaxian et al., 1997). Degassing and cooling rates, as well as geochemical evidence (Walker et al., 1993), suggest that this upper reservoir must, at least periodically, be recharged from a deeper source.

The significant observed gravity decreases clearly imply thickening of a gas-rich layer. Subsequent gas flux decreases may be due to trapping and storage of this gas in a zone immediately beneath San Pedro and the other craters. Pressure increase or cavern unroofing may then permit gas to escape and allow the craters to develop further. The sudden increase in the thickness of a low-density layer may indicate an increase in the gas supply rate to a level greater than that at which the gas can escape. Thus, gravity change may actually predict changes in gas flux, which has serious implications for hazard mitigation at persistently active volcanoes. Crucially, there must be 1) a region where gas can be trapped and accumulate, 2) variable gas input from below and 3) limited space for the gas to escape. This has significant implications for the understanding of other volcanoes. At volcanoes such as Poás, Costa Rica the gas release would be seriously restricted by the highly developed hydrothermal systems allowing for accumulation and development of a low-density zone. On the other hand, at volcanoes with relatively open vents (e.g., Stromboli and Mt. Etna, Italy), the gas might escape more easily and thus not accumulate to the point where a significant density decrease within the shallow plumbing system would be visible.

The integration of micro-gravity and COSPEC measurements over an extended period of time allows for a better understanding of persistent volcanism. Recent activity at Masaya (1993-present) is characterised by repeated fluctuations in micro-gravity and gas flux and is likely to be due the formation and oscillation of a gas-rich vesiculated zone immediately beneath the San Pedro, Nindirí and Santiago craters. Four stages of activity within the most current degassing episode have been identified, with the most recent data suggesting that the system may be entering another period of reduced degassing. The cyclical nature of the observed variations in micro-gravity and gas flux and lack of any significant gravity increase or deformation discount intrusion of new magma into the shallow magmatic system. Rather, it necessitates either the blocking and accumulation of gas due to restrictions in the volcano

substructure or the convective overturn of shallow, pre-existing, degassed, cooled, dense magma that is replaced periodically by lower density, hot, gas-rich magma from depth. The observed surface anomalies may also be due to a combination of both processes. Nevertheless, it is clear that these are continuous processes that occur at shallow levels immediately beneath the craters as well as at depth in the magma reservoir.

Acknowledgements

This research was supported by the Royal Society, The Open University Research Development Fund and NERC. We greatly appreciate the help of all the staff at the Parqué Nacional de Masaya and INETER-Geofisica, especially M. Navarro, W. Straugh, J. Alvarez, L. Acosta, A. Acosta, and O. Canales. Field work was greatly facilitated by the help of A. Beaulieu, N. Fournier, S. La Monica, I. Lépine, G. Maton, J.-M. Séguin, B. Williams-Jones and W.D. Whitaker.

References

Berrino, G., Corrado, G., Luongo, G., Toro, B., 1984. Ground deformation and gravity changes accompanying the 1982 Pozzuoli uplift. Bull. Volcanol. 47, 187-200.

BGVN, 1970-2001. Masaya. Bulletin of the Global Volcanism Network, Smithsonian Institute 38:70-26:04.

BGVN, 2000. Masaya. Bulletin of the Global Volcanism Network, Smithsonian Institute 15:09.

BGVN, 2001. Masaya. Bulletin of the Global Volcanism Network, Smithsonian Institute 26:04.

Broucke, R.A., Zürn, W.E., Slichter, L.B., 1972. Lunar tidal acceleration on a rigid earth, Flow and Fracture of Rocks. Am. Geophys. Union, Geophysical Monograph 319-324.

Carbone, D., Rymer, H., 1999. Calibration shifts in a LaCoste-and-Romberg gravimeter; comparison with a Scintrex CG-3M. Geophys. Prospect. 47, 73-83.

Casadevall, T.J., Stokes, J.B., Greenland, L.P., Malinconico, L.L., Casadevall, J.R.Furukawa, B.T., 1987. SO_2 and CO_2 emission rates at Kilauea Volcano, 1979-1984. In: Decker, R.W., Wright, T.L., Stauffer, P.H. (Eds.), Volcanism in Hawaii. U. S. Geol. Surv. Prof. Paper, pp. 771-780.

Davies, M.A., Harrop, N.D., Rymer, H., 2000. Experimental investigation of temporary tares induced by ground vibration in LaCoste and Romberg gravity meters. Geophys. Prospect. In press.

Delmelle, P., Baxter, P., Beaulieu, A., Burton, A., Francis, P., Garcia-Alvarez, J., Horrocks, L., Navarro, M., Oppenheimer, C., Rothery, D., Rymer, H., St. Amand, K., Stix, J., Strauch, W.Williams-Jones, G., 1999. Origin, effects of Masaya volcano's continued unrest probed in Nicaragua. EOS Trans. Am. Geophys. Union 80, 575-581.

Denlinger, R.P., 1997. A dynamic balance between magma supply and eruption rate at Kilauea volcano, Hawaii. J. Geophys. Res. 102, 18091-18100.

Francis, P., Oppenheimer, C., Stevenson, D., 1993. Endogenous growth of persistently active volcanoes. Nature 366, 554-557.

Gauthier, P.-J., Le Cloarec, M.-F., Condomines, M., 2000. Degassing processes at Stromboli volcano inferred from short-lived disequilibria (210Pb-210Bi-210Po) in volcanic gases. J. Volcanol. Geotherm. Res. 102, 1-19.

Harris, A.J.L., Flynn, L.P., Rothery, D.A., Oppenheimer, C., Sherman, S.B., 1999. Mass flux measurements at active lava lakes: Implications for magma recycling. J. Geophys. Res. 104, 7117-7136.

Jachens, R.C., Roberts, C.W., 1985. Temporal and areal gravity investigations at Long Valley Caldera, California. J. Geophys. Res. 90, 11210-11218.

Jaupart, C., Vergniolle, S., 1989. The generation and collapse of a foam layer at the roof of a basaltic magma chamber. J. Fluid Mech. 203, 347-380.

Jousset, P., Dwipa, S., Beauducel, F., Duquesnoy, T., Diament, M., 2000. Temporal gravity at Merapi during the 1993-1995 crisis: an insight into the dynamical behaviour of volcanoes. J. Volcanol. Geotherm. Res. 100, 289-320.

Kazahaya, K., Shinohara, H., Saito, G., 1994. Excessive degassing of Izu-Oshima volcano: magma convection in a conduit. Bull. Volcanol. 56, 207-216.

Krásný, J., Hecht, G., 1998. Estudios Hidrogeológicos e Hidroquímicos de la Región del Pacífico de Nicaragua, INETER-Hidrogeología, Managua.

McBirney, A.R., 1956. The Nicaraguan volcano Masaya and its caldera. EOS Trans. Am. Geophys. Union 37, 83-96.

Métaxian, J.-P., 1994. Étude Sismologique et Gravimétriqe d'un Volcan Actif: Dynamisme Interne et Structure de la Caldera Masaya, Nicaragua, Université de Savoie, France, 319 pp.

Métaxian, J.-P., Lesage, P., Dorel, J., 1997. Permanent tremor of Masaya Volcano, Nicaragua: Wave field analysis and source location. J. Geophys. Res. 102, 22529-22545.

Métrich, N., Schiano, P., Clocchiatti, R., Maury, R.C., 1999. Transfer of sulfur in subduction settings: an example from Batan Island (Luzon volcanic arc, Philippines). Earth Planet. Sci. Lett. 167, 1-14.

Millán, M.M., 1980. Remote sensing of air pollutants. A study of some atmospheric scattering effects. Atmos. Environ. 14, 1241-1253.

Murray, J.B., Pullen, A.D., Saunders, S., 1995. Ground deformation surveying of active volcanoes. In: McGuire, B., Kilburn, C.R.J., Murray, J. (Eds.), Monitoring Active Volcanoes. UCL Press, London, pp. 113-150.

Pedley, R., 1991. Gravmag user manual. Integrated Geophysical Services, BGS Keyworth, UK.

Pyle, D.M., 1992. The volume and residence time of magma beneath active volcanoes determined by decay-series disequilibria methods. Earth Planet. Sci. Lett. 112, 61-73.

Roggensack, K., Hervig, R.L., McKnight, S.B., Williams, S.N., 1997. Explosive basaltic volcanism from Cerro Negro volcano: influence of volatiles on eruptive style. Science 277, 1639-1642.

Rymer, H., 1994. Microgravity change as a precursor to volcanic activity. J. Volcanol. Geotherm. Res. 61, 311-328.

Rymer, H., 1996. Microgravity monitoring. In: Scarpa, R., Tilling, R.I. (Eds.), Monitoring and Mitigation of Volcano Hazards. Springer-Verlag, Berlin, pp. 169-198.

Rymer, H., Brown, G.C., 1989. Gravity changes as a precursor to volcanic eruptions at Poás volcano, Costa Rica. Nature 342, 902-905.

Rymer, H., Cassidy, J., Locke, C.A., Murray, J.B., 1995. Magma movements in Etna volcano associated with the major 1991-1993 lava eruption: evidence from gravity and deformation. Bull. Volcanol. 57, 451-461.

Rymer, H., van Wyk de Vries, B., Stix, J., Williams-Jones, G., 1998. Pit crater structure and processes governing persistent activity at Masaya Volcano, Nicaragua. Bull. Volcanol. 59, 345-355.

Stevenson, D.S., Blake, S., 1998. Modelling the dynamics and thermodynamics of volcanic degassing. Bull. Volcanol. 60, 307-317.

Stoiber, R.E., Malinconico, J.L.L., Williams, S.N., 1983. Use of the correlation spectrometer at volcanoes. In: Tazieff, H., Sabroux, J.C. (Eds.), Forecasting Volcanic Events. Elsevier, New York, pp. 424-444.

Stoiber, R.E., Williams, S.N., Huebert, B.J., 1986. Sulfur and halogen gases at Masaya caldera complex, Nicaragua: Total flux and variations with time. J. Geophys. Res. 91, 12215-12231.

Telford, W.M., Geldart, L.P., Sheriff, R.E., 1990. Applied Geophysics. Cambridge University Press, Cambridge, U.K., 770 pp.

van Wyk de Vries, B., 1993. Tectonics and magma evolution of Nicaraguan volcanic systems. Ph.D. Thesis, The Open University,, Milton Keynes, U.K., 328 pp.

Walker, J.A., Williams, S.N., Kalamarides, R.I., Feigenson, M.D., 1993. Shallow open-system evolution of basaltic magma beneath a subduction zone volcano: the Masaya Caldera Complex, Nicaragua. J. Volcanol. Geotherm. Res. 56, 379-400.

Williams, S.N., 1983a. Geology and eruptive mechanisms of Masaya Caldera Complex, Nicaragua. Ph.D. Thesis, Dartmouth College, Hanover, New Hampshire, 169 pp.

Williams, S.N., 1983b. Plinian airfall deposits of basaltic composition. Geology 11, 211-214.

Williams-Jones, G., 2001. Integrated Geophysical Studies at Masaya Volcano, Nicaragua. Ph.D. Thesis, The Open University, Milton Keynes, 237 pp.

Williams-Jones, G., Stix, J., Hickson, C.J., In Press. Using the COSPEC in the field. In: Stix, J., Hickson, C.J. (Eds.), Theory, use, and application of the COSPEC correlation spectrometer at active volcanoes. Geol. Surv. Can. Bull.

Yokoyama, I., 1989. Microgravity and height changes caused by volcanic activity: four Japanese examples. Bull. Volcanol. 51, 333-345.

Tables

Table 1: Elevation (m a.s.l.) of stations in the micro-gravity network between October 1994 and February 2001.

Station	Oct-94	Mar-96	Mar-97	Jan-98	Feb-98	Mar-98	Feb-99	Mar-99	Mar-00	Feb-01	S.D. (cm)
A1	302.11	302.11	302.11	302.11	302.11	302.11	302.11	302.11	302.11	302.11	0.0
A2	295.59	295.58			295.53		295.60		295.61		3.1
A3	297.78	297.77		297.83	297.75		297.82		297.80		2.9
A4	319.70	319.68			319.64		319.70		319.70		2.5
A5	365.73	365.85	365.81								6.0
A6	439.13						439.15		439.13		1.4
A7	520.73		520.75	520.83	520.71		520.79		520.81	520.80	4.2
A8	565.92	565.96	565.93	566.00	565.91		565.99		565.99		3.7
A9	511.88	511.92	511.89			511.87	511.96		511.95		3.9
A10	509.09	509.13		509.19	509.09		509.19				4.9
A11			503.21	503.27	503.16		503.26		503.24		3.8
Arenal					281.96			282.04	282.09		6.5
B1a		525.48	525.49	525.56	525.45						4.4
B2	524.79	524.78	524.78	524.83	524.75		524.81		524.85	524.79	3.1
Coyotes	284.69				284.62		284.71		284.75		5.4
Coyotes2					236.66						
E1	587.72			587.77	587.68		587.78		587.77		4.4
E3	509.51		509.55	509.61	509.51		509.60		509.58		4.1
E4	517.36	517.37		517.43	517.33		517.40		517.42		3.8
Edge				519.82	519.70		519.76		519.77		4.7
Fence2							123.86		123.84		1.7
Flanco					492.28		492.34		492.35		3.5
Laguna					118.51		118.66		118.64		8.4
Laguna2					130.29		130.35		130.35		3.1
Montoso					287.63				287.63		0.5
Muertes					198.99		199.08				5.8
MurodeLava					454.72		454.79		454.78		3.8
Museo				310.12			310.10	310.10			1.2
Nindirí						485.31	485.30		485.33		1.2
Pedro			517.08	517.13			517.10		517.08		2.0
Pedro2					520.13		520.18		520.20		3.9
Sismo					589.56		589.60		589.64		3.8
									Average S.D.		**3.6**
									Average S.D. summit:		**3.7**

Station A1 was levelled precisely in 1993 by J.B. Murray (Rymer et al., 1998) and is used as a benchmark from which all other stations are referenced. Note that, due to technical difficulties, there is a complete lack of data for September 1999, June 1999 and April 2000 and only limited data for March 1998, March 1999 and February 2001.

Table 2: SO_2 and Total gas flux, estimated magma degassing rate and calculated gravity change from Masaya, 1993-2001.

Degassing period	SO_2 flux (kg yr^{-1})	Total gas flux (kg yr^{-1})	Magma degassing rate (kg yr^{-1}) Assuming initial melt S concentrations			*Mass change calculated from gravity change (kg)
			270 ppm	800 ppm	1500	
93-94	2.2×10^8	4.7×10^9	4.1×10^{11}	1.4×10^{11}	7.3×10^{10}	-2.2×10^9
94-97	2.0×10^8	4.3×10^9	3.7×10^{11}	1.3×10^{11}	6.7×10^{10}	
97-99	4.8×10^8	1.0×10^{10}	8.9×10^{11}	3.0×10^{11}	1.6×10^{11}	-2.1×10^9
98-99	6.5×10^8	1.4×10^{10}	1.2×10^{12}	4.0×10^{11}	2.2×10^{11}	-1.4×10^9
99-01	4.7×10^8	1.0×10^{10}	8.8×10^{11}	3.0×10^{11}	1.6×10^{11}	

*Calculated using Gauss' theorem, see Equation 2.

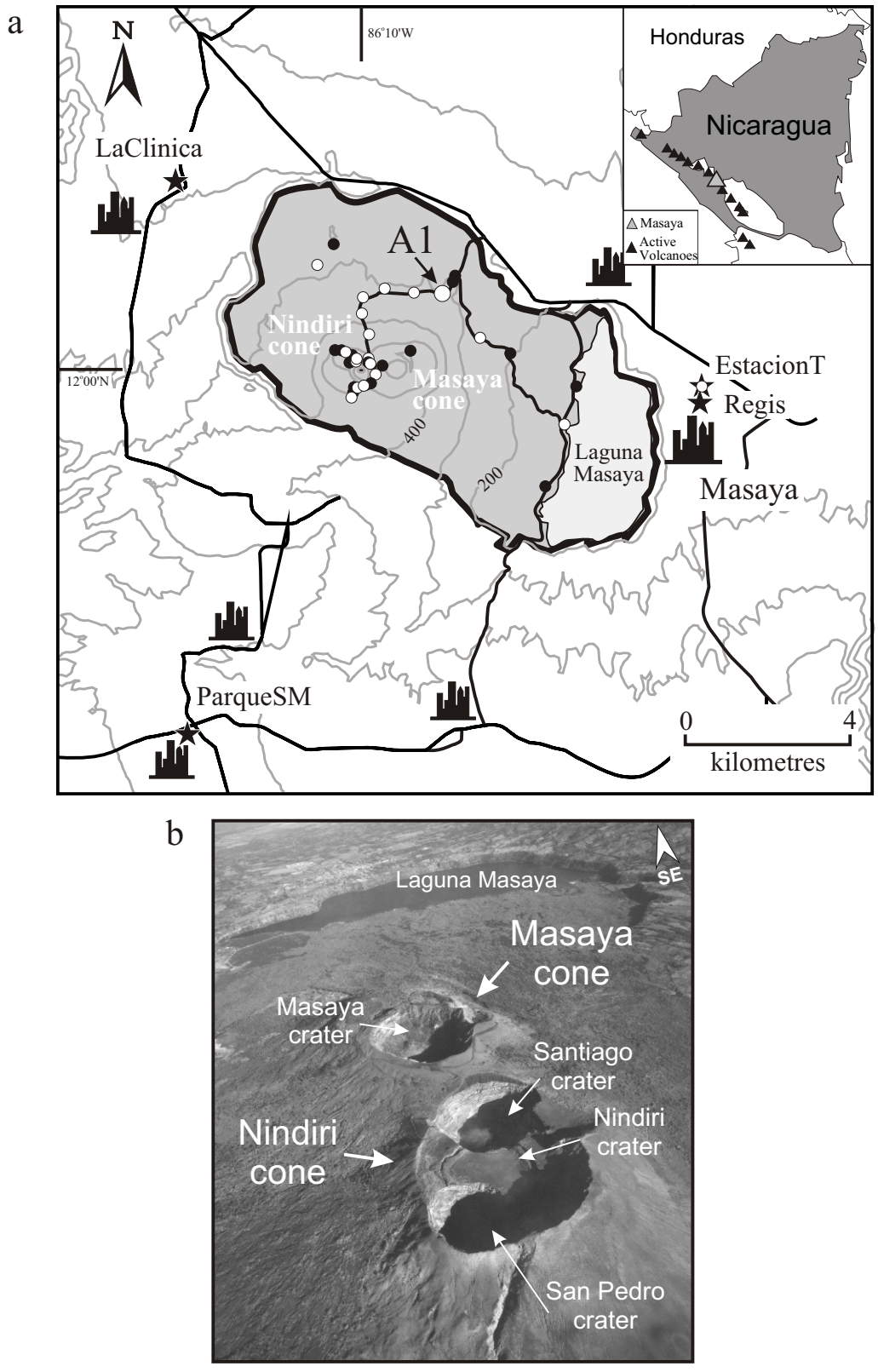

Figure 1: a) Masaya caldera (shaded area) with the inter-caldera gravity/GPS stations (small black or white dots) and extra-caldera reference stations (black stars). White dots show stations where Free-Air Gradient measurements were also made. All gravity measurements are quoted relative to station A1 (large white dot). Contours are 100 m. Inset map indicates Masaya (grey triangle) and the active volcanoes (black triangles) of the Central American Volcanic Front. b) Aerial view of Masaya and Nindiri cones from the northwest.

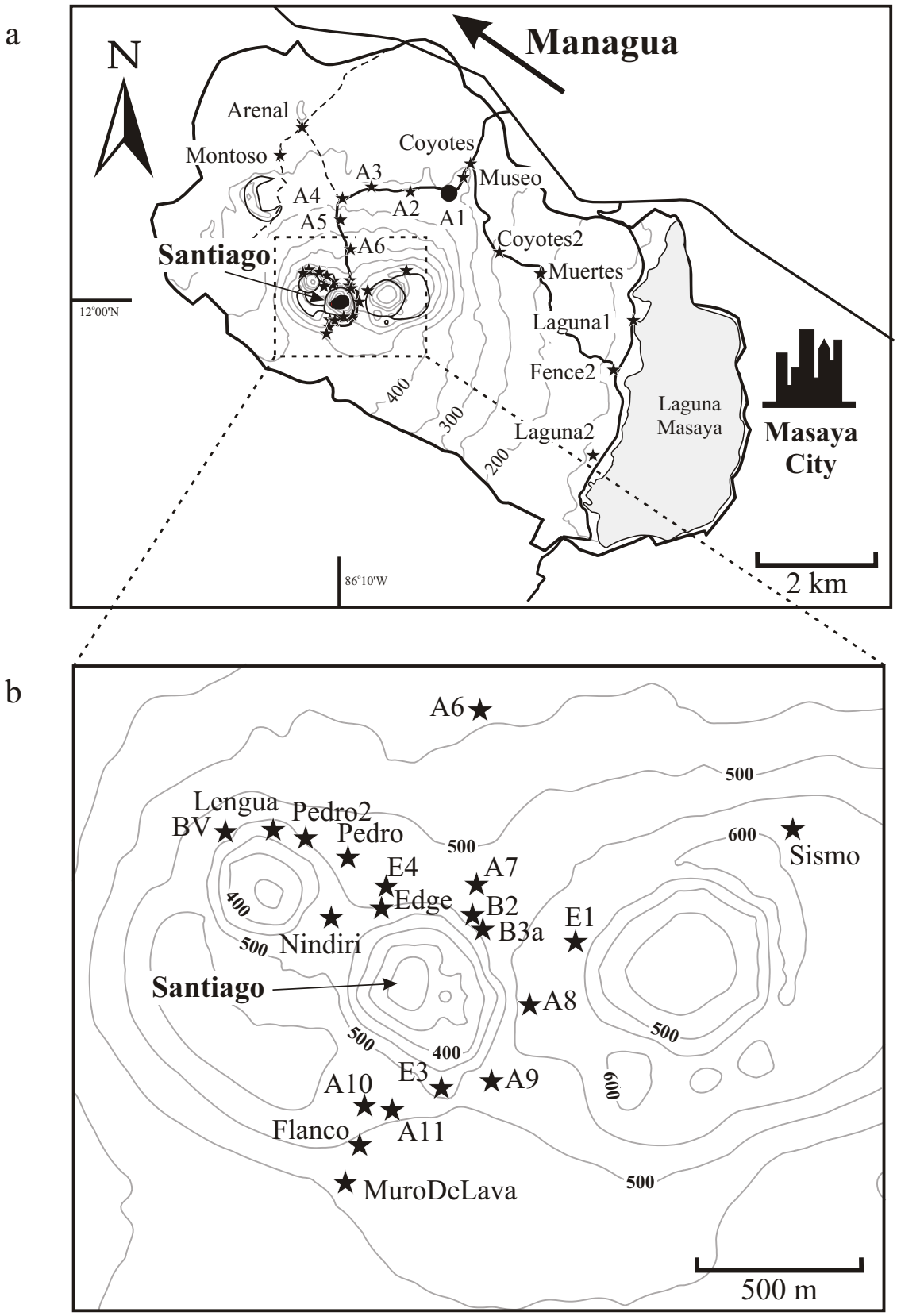

Figure 2: Map of a) the distal (>2 km from Santiago crater) and b) proximal inter-caldera gravity/GPS stations (black stars). Black dot is the reference base station A1. Contour interval is 50 m.

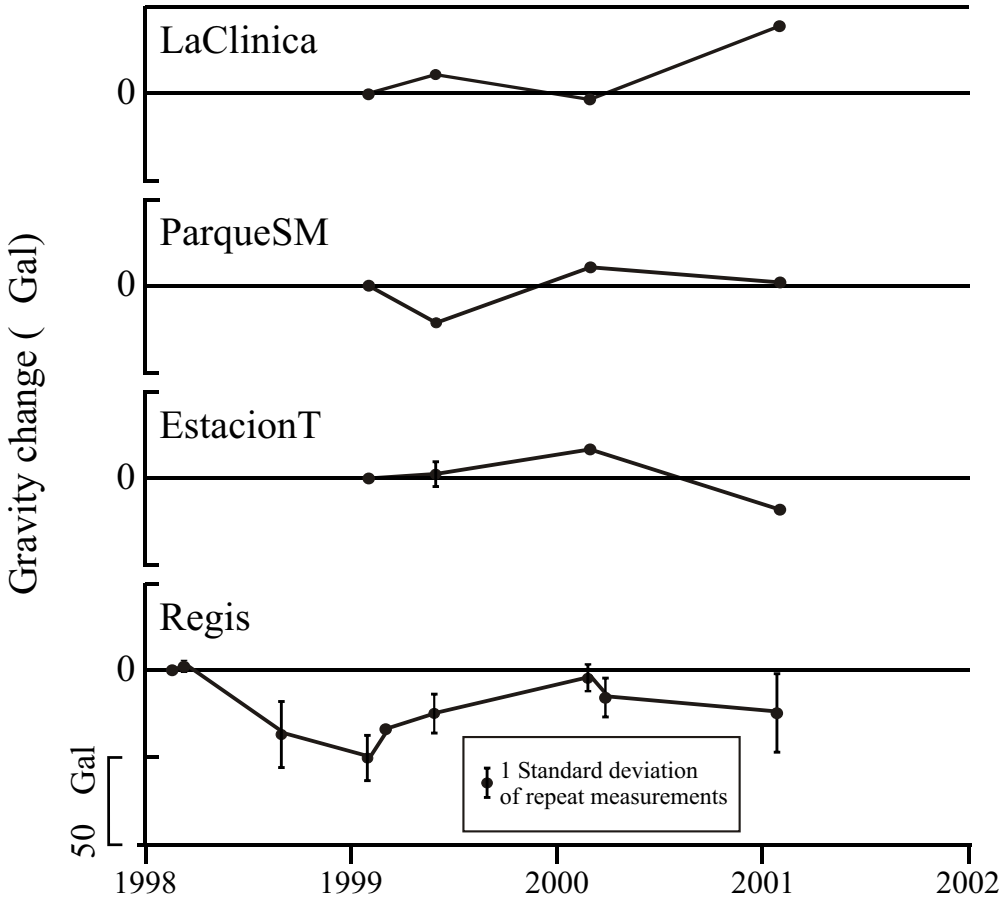

Figure 3: Gravity changes at 4 reference stations outside the caldera (relative to A1). See Figure 1 for station locations. These stations were only added to the gravity/GPS network in 1998 (Regis) and 1999 (LaClinica, ParqueSM, EstacionT).

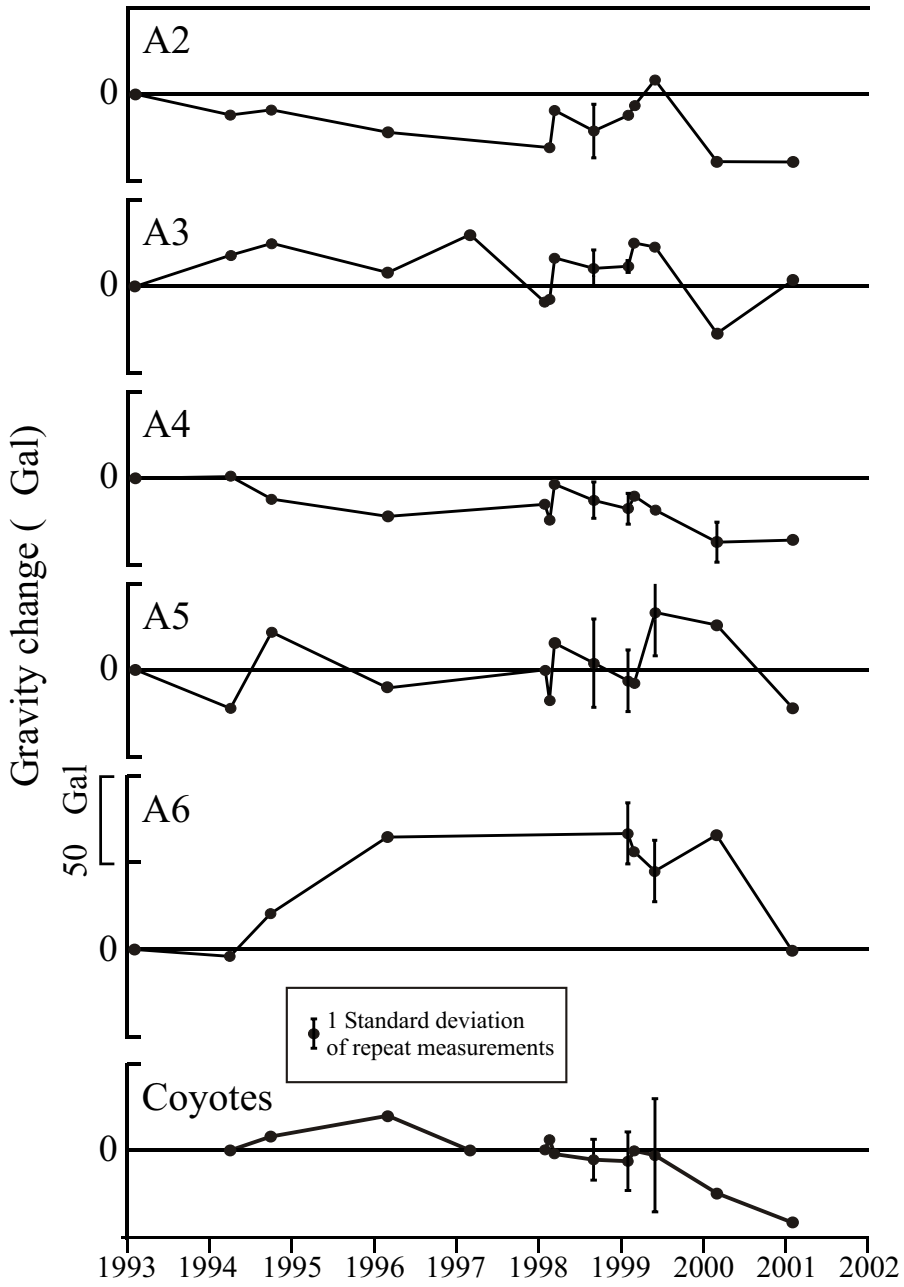

Figure 4: Gravity changes at representative distal stations (>2 km from summit) quoted relative to A1. The apparently large gravity change at station A6 between 1994 and 1996 is likely due to a poor initial measurement. See Figure 2 for station locations.

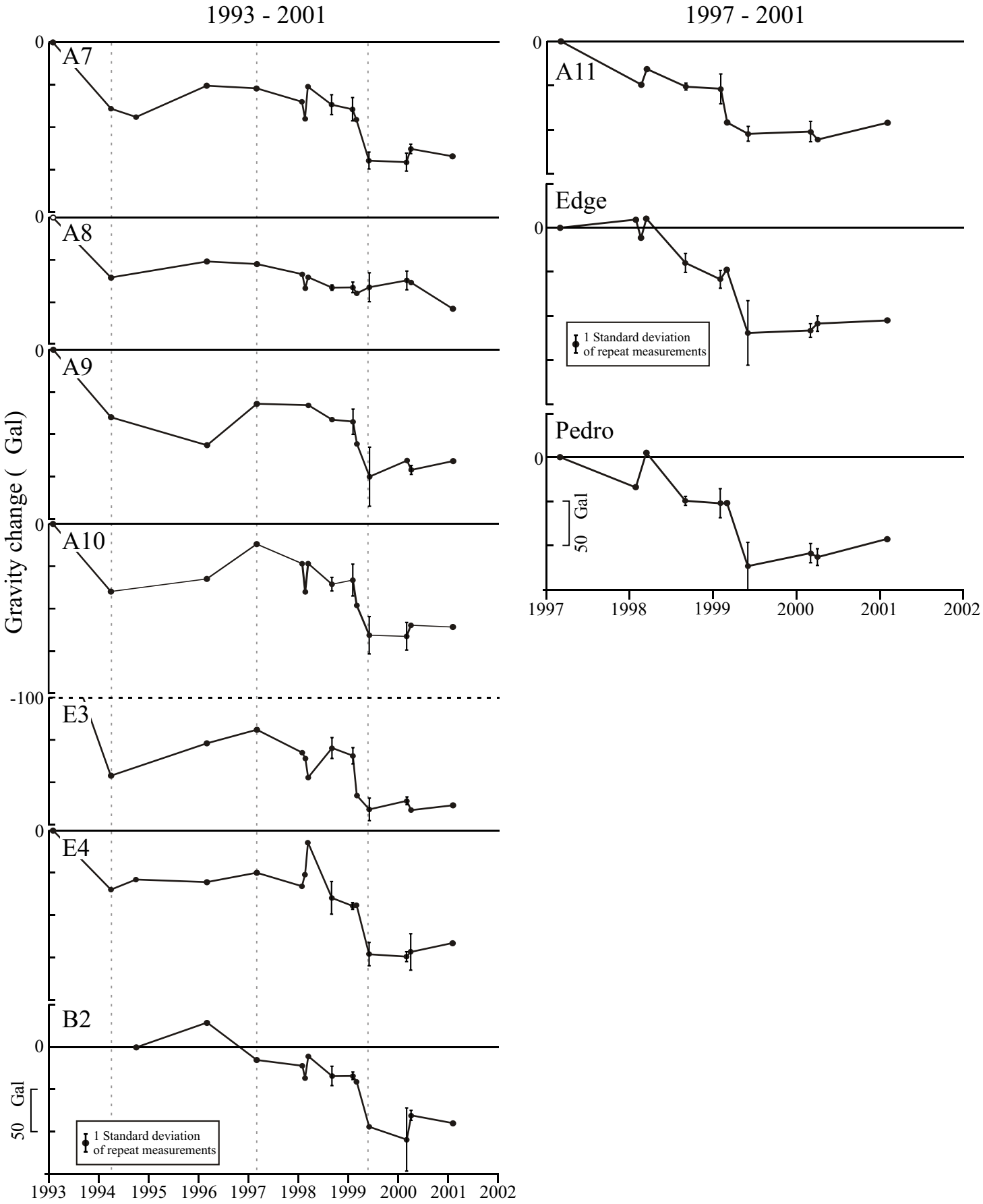

Figure 5: Monthly average gravity changes at summit stations between 1993 and 2001 (quoted relative to station A1). Stations A11, Edge, and Pedro were not present in 1993. Dashed line highlights the end and beginning of the 1993-1994 and 1997-1999 periods of

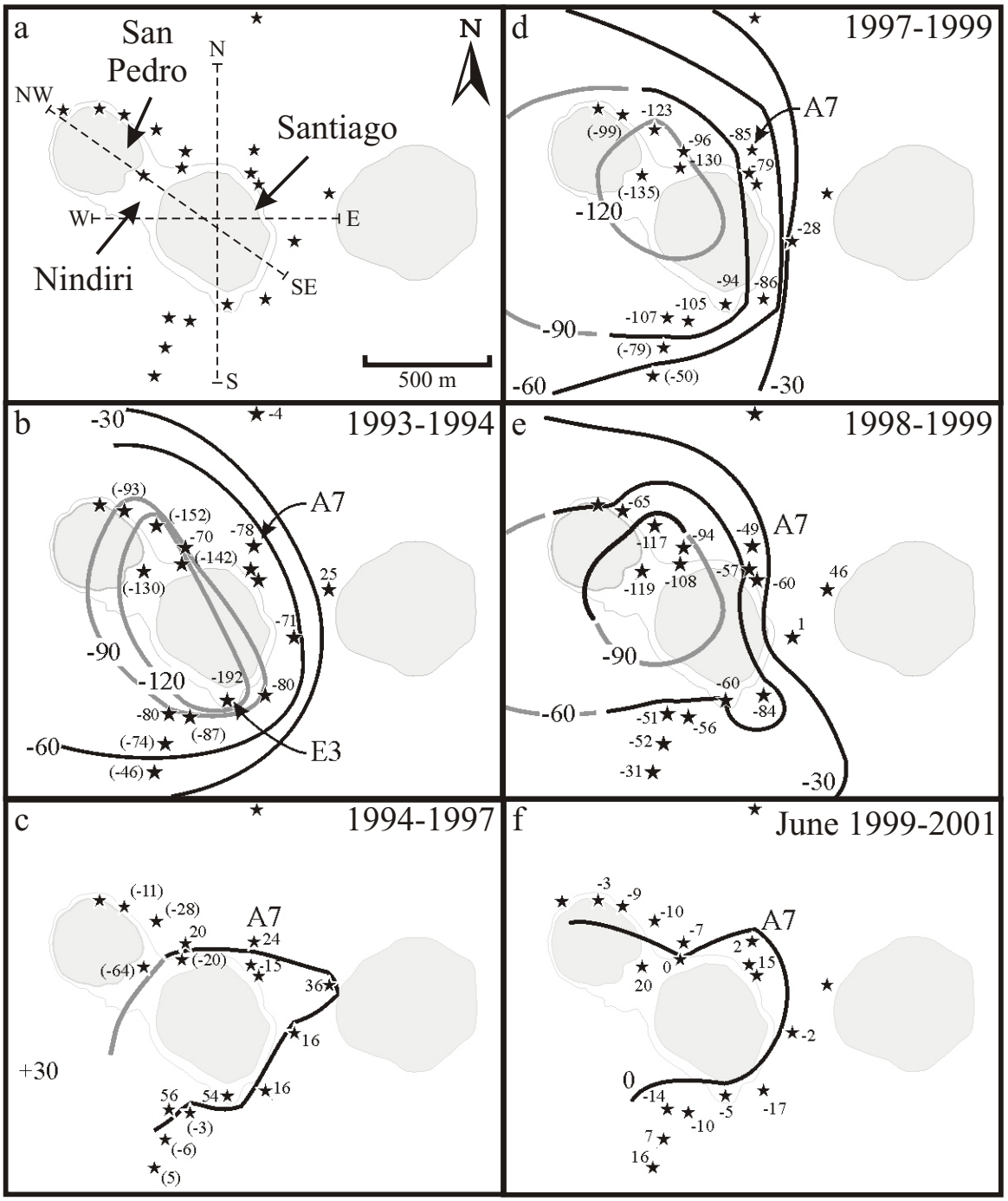

Figure 6: Schematic contour maps of approximate gravity change through time. Two episodes of gravity decrease are shown in (b) 1993-1994 and (d) 1997-1999 while periods of gravity increase are shown in (c) 1994-1997 and (f) 1999-2001.
Numbers at stations indicate gravity changes for each station quoted relative to A1. Numbers in parentheses are estimated values (explained in the text). Grey contours are based on estimated values. Contour interval is 30 Gal. Dashed lines in (a) represent NS, WE and NW-SE profiles for Figure 8. Station A7 is identified in (b) through (f) for reference.

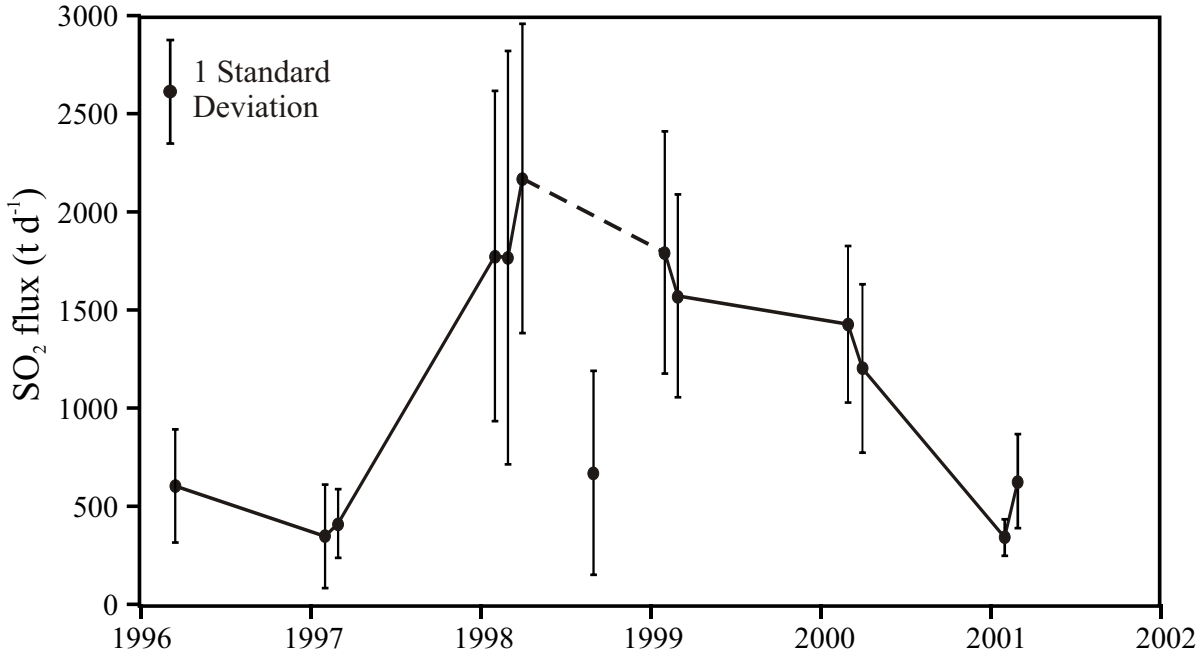

Figure 7: Average monthly SO_2 flux measured downwind from Santiago crater. Black circles represent an average of 43 measurements (ranging from 8 to 99 measurements) for a given month, where a measurement is one complete transect beneath the plume. Note that the measurements in September 1998, the only wet season data on this plot, are probably anomalous due to environmental effects (rain and low wind speeds) and are not considered representative.

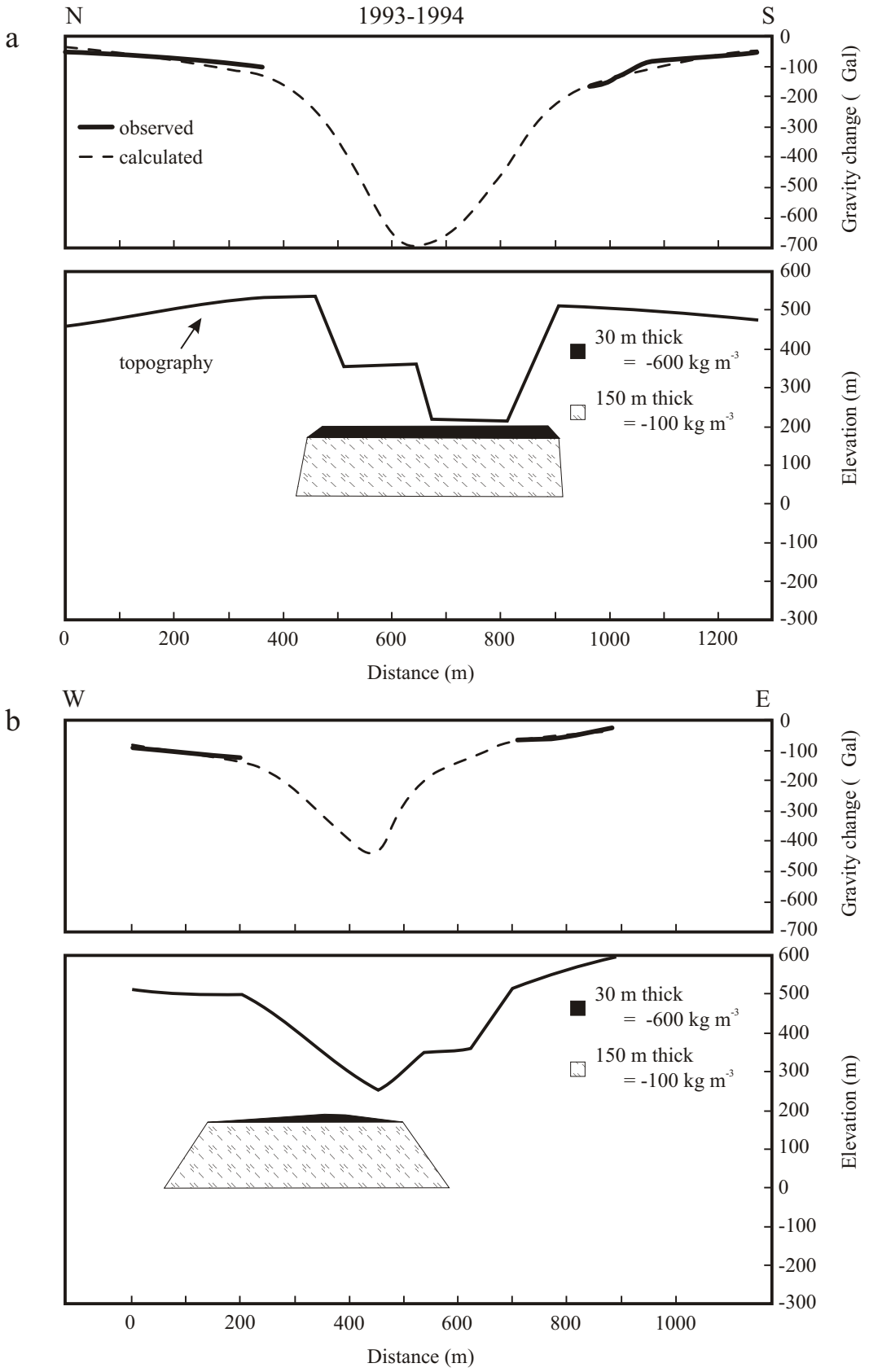

Figure 8: Observed and calculated gravity changes and density changes in a modelled causative body for the a) north-south and b) west-east profile of the 1993-1994 gravity decrease. Modelled bodies have thicknesses of 30 and 150 m with density changes of -600 and -100 kg m^{-3}, respectively. All bodies have a constant half strike of 200 m. Profiles from Figure 6a.

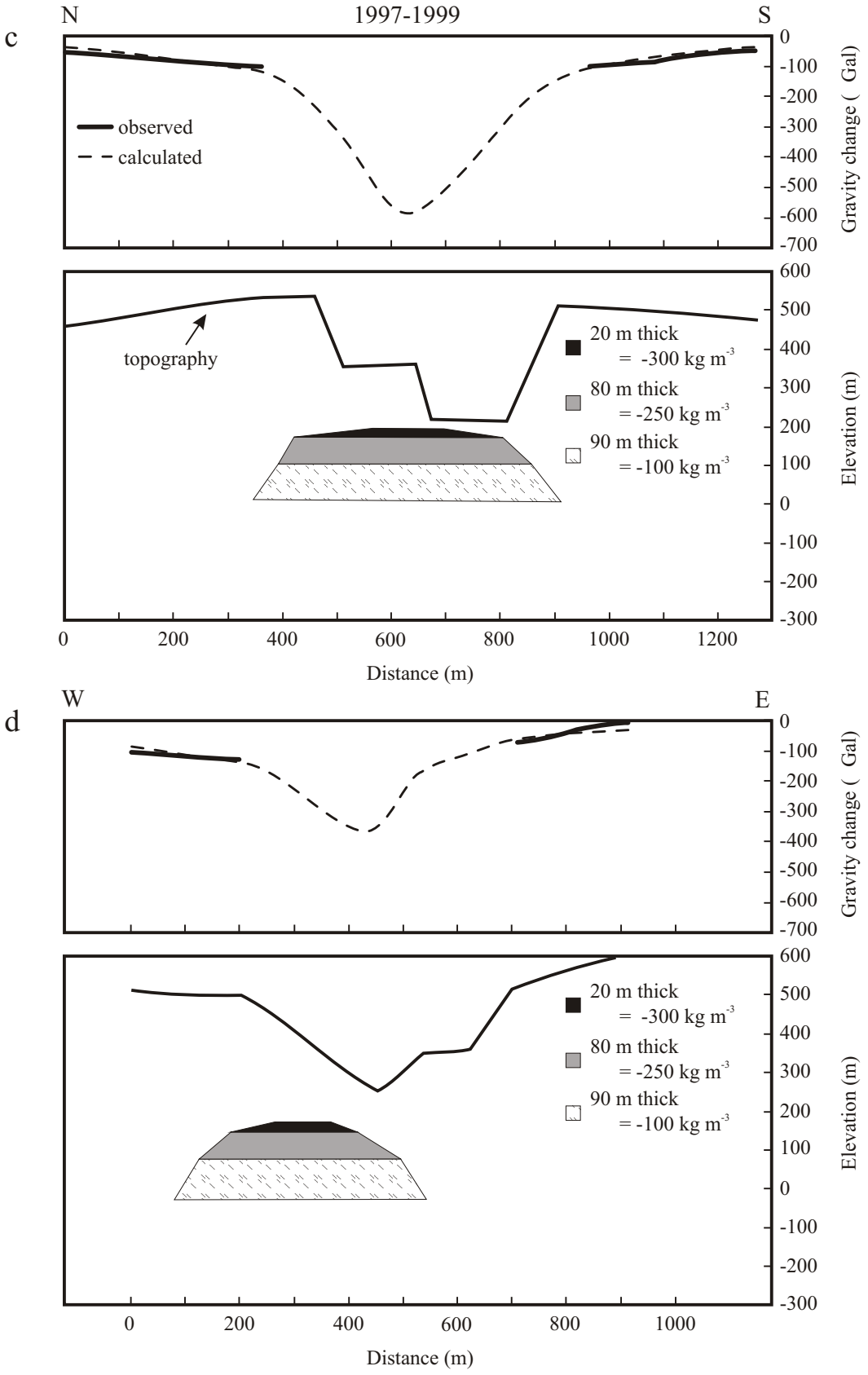

Figure 8 - Continued: Observed and calculated gravity changes and density changes in a modelled causative body for the c) north-south and d) west-east profile of the 1997-1999 gravity decrease. Modelled bodies have thicknesses of 20, 70 and 90 m with density changes of -300, -250 and -100 kg m^{-3}, respectively. All bodies have a constant half strike of 200 m. Profiles from Figure 6a.

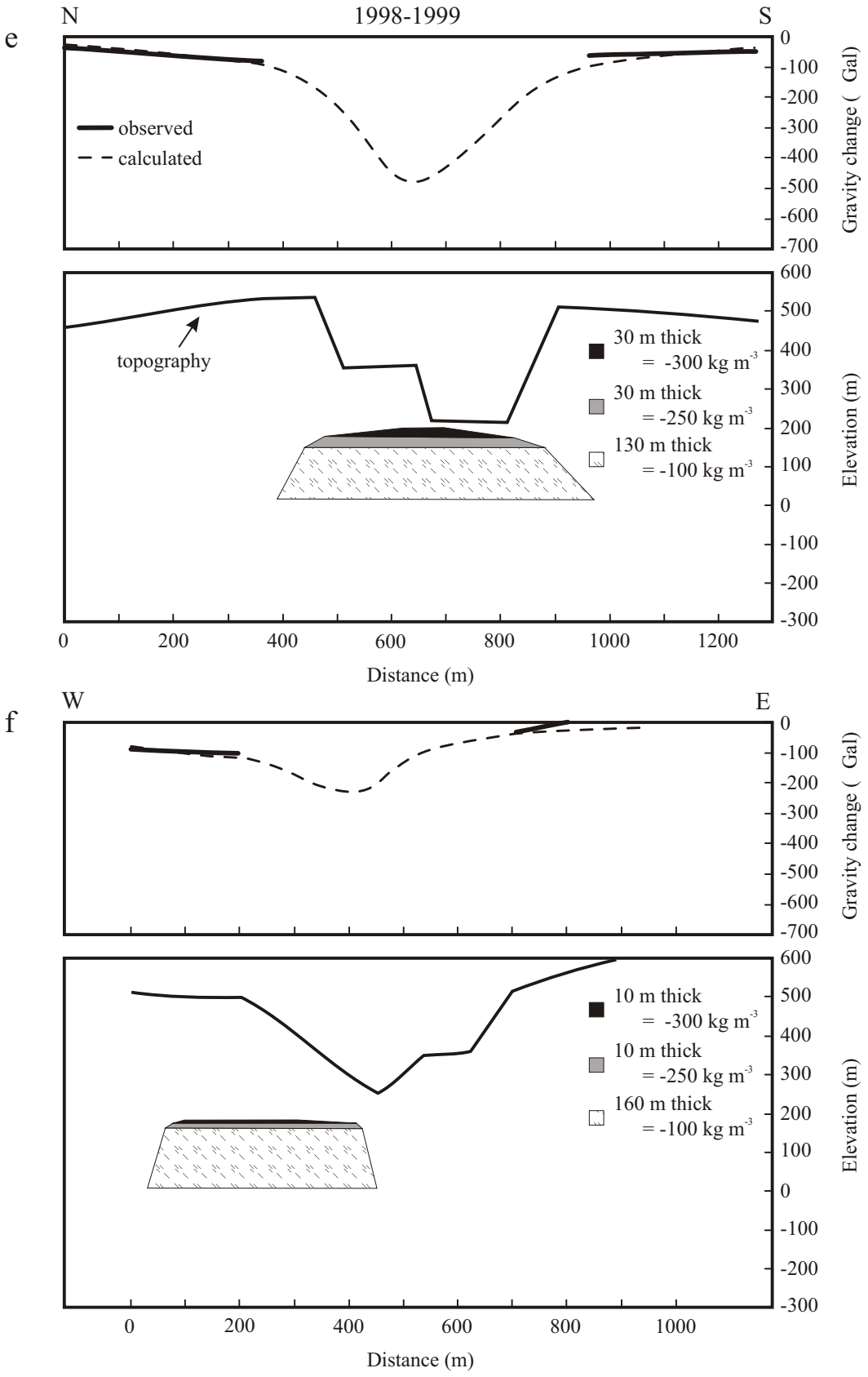

Figure 8 - Continued: Observed and calculated gravity changes and density changes in a modelled causative body for the e) north-south and f) west-east profile of the 1998-1999 gravity decrease. All bodies have a constant half strike of 200 m. Profiles from Figure 6a.

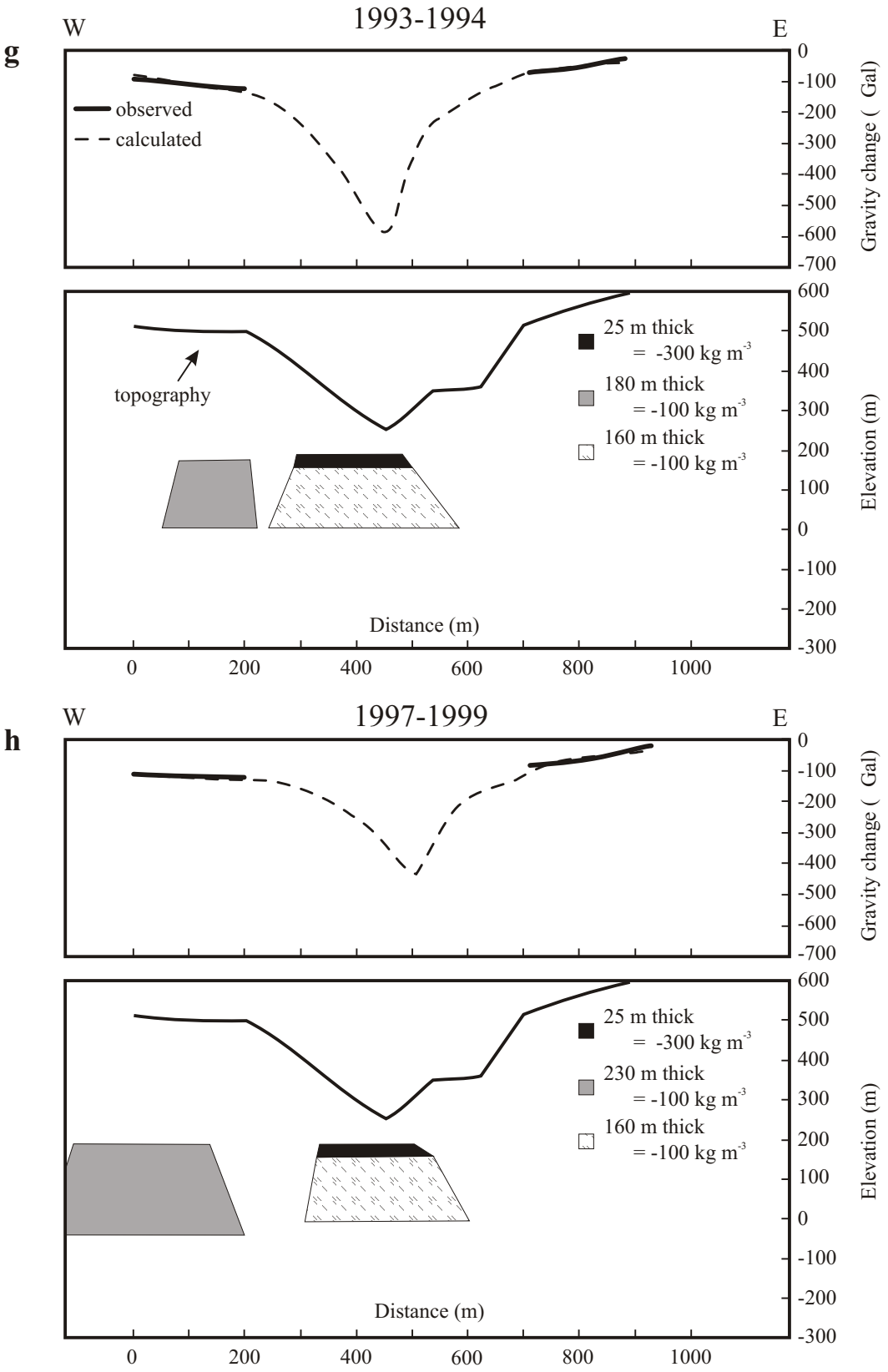

Figure 8 - Continued: Observed and calculated gravity changes and density changes in a modelled causative bodies for the west-east profile of the g) 1993-1994 and h) 1997-1999 gravity decreases. Note that the grey and hatched bodies are the same density change. All bodies have a constant half strike of 200 m. Profiles from Figure 6a.

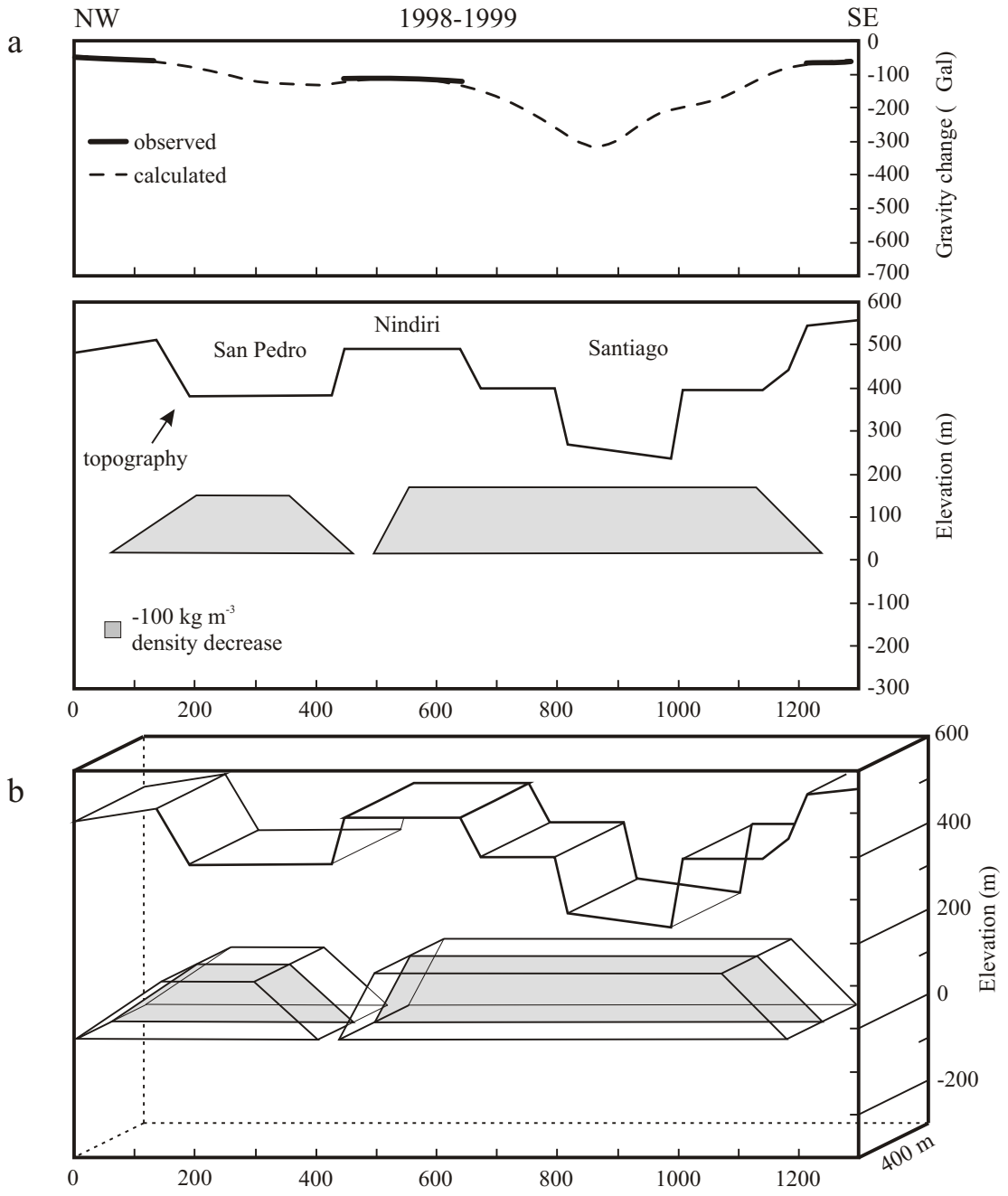

Figure 9: a) Observed and calculated gravity changes and density changes in a modelled causative body for the northwest-southeast profile of the 1998-1999 gravity decrease. b) Perspective view shows the 2.5D modelled bodies with a symmetrical 200-m half strike. Profiles from Figure 6a.

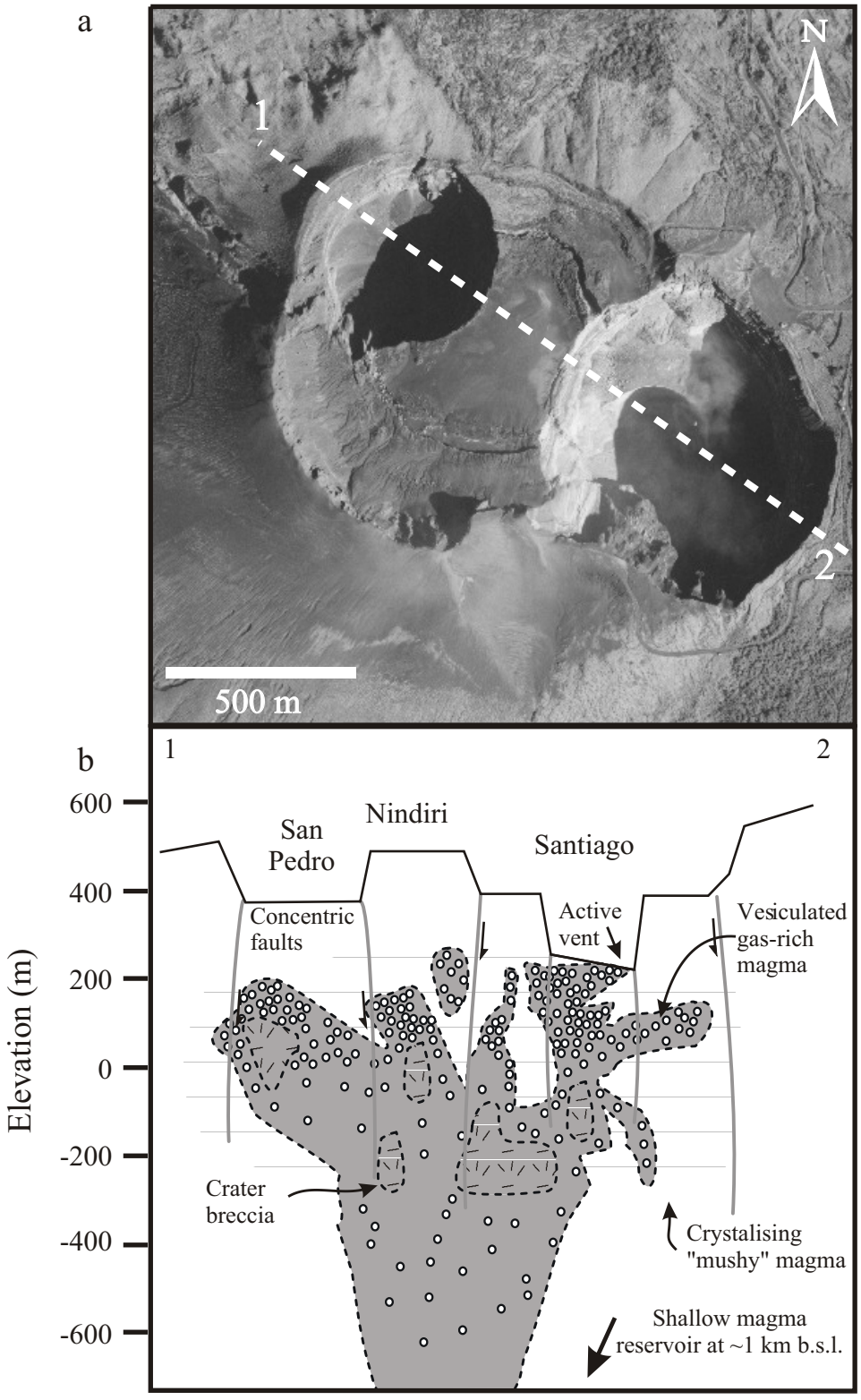

Figure 10: a) Aerial photo and b) schematic cross-section (profile 1-2, from left to right) of San Pedro, Nindiri and Santiago pit craters. The location of the proposed zone of vesiculated gas-rich magma is based on the gravity models. The crystallising "mushy" magma is purely conceptual. Concentric faults are inferred from observed structure and collapse history. *Modified after Rymer et al., 1998.*

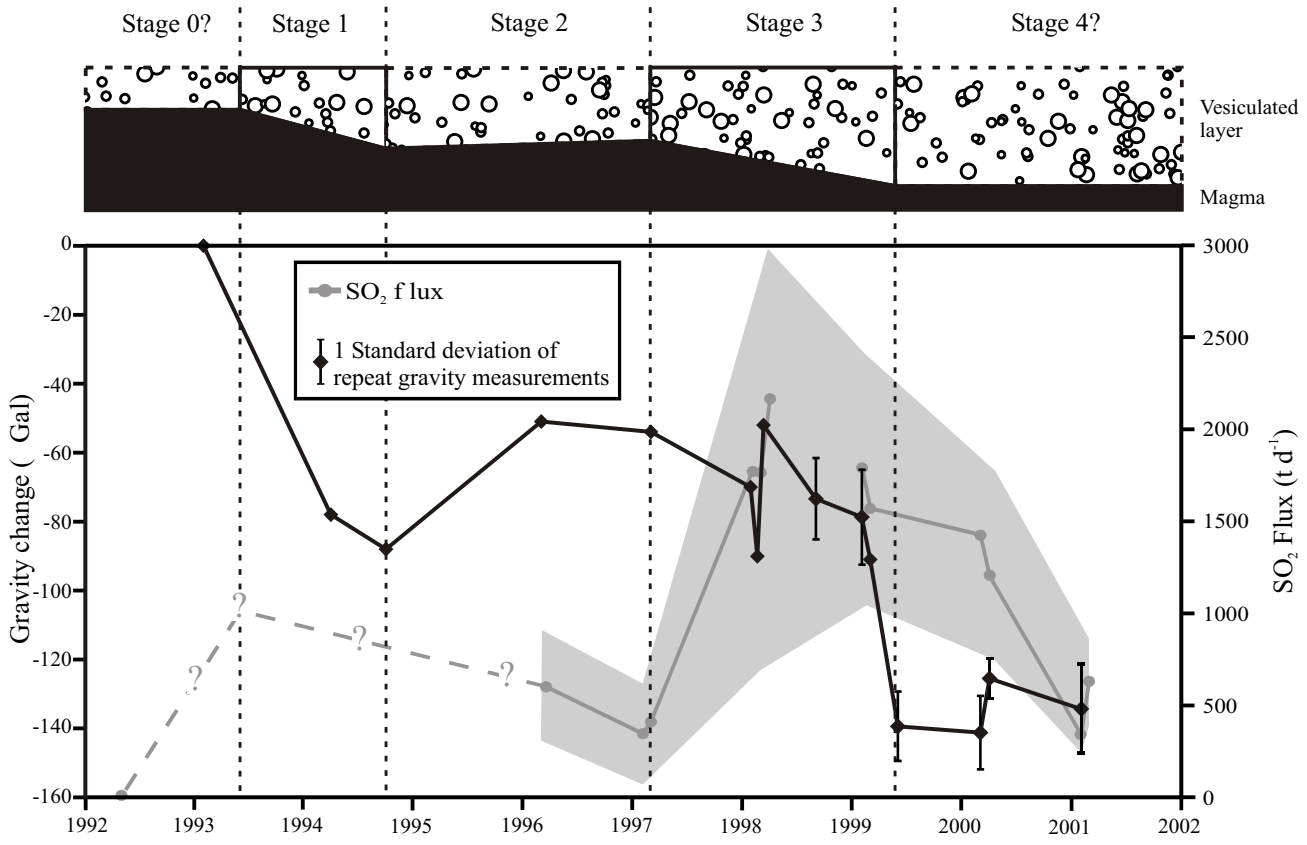

Figure 11: Average monthly gravity change (black diamonds) at a representative crater rim station (A7) compared with average monthly SO_2 flux (grey circles) at Masaya. Grey shaded region represents one standard deviation of SO_2 flux values (~30%). Dashed lines denote the five stages of activity between 1992 and 2001. The schematic cross-section illustrates the possible stages of thinning and thickening of the vesiculated gas-rich layer due to changes in gas flux. The top of this layer corresponds to the roof of the vesiculated zone in Figure 10b. Boxes represent the ~200 m thick layer (gravity modelled for Stage 1 and 3). Dashed boxes are unmodelled.